

Supplemental Materials

Methods

Ethics statement. Animals used in the high fat diet study were housed at the University of Pittsburgh animal facilities, in accordance with the recommendations of the Association for Assessment and Accreditation of Laboratory Animal Care (AAALAC) International, and with the recommendations included in the Guide for the Care and Use of Laboratory Animals of the National Institutes of Health. Efforts were made to minimize nonhuman primate (NHP) suffering, in agreement with the recommendations of the Weatherall report, "*The use of nonhuman primates in research*". The NHP facility is air-conditioned, with an ambient temperature of 21-25°C, a relative humidity of 40-60% and a 12 h light/dark cycle. Animals were housed in suspended stainless-steel wire-bottomed cages. A variety of environmental enrichment strategies were employed including providing toys to manipulate and playing entertainment videos in the animal rooms. In addition, the NHPs were observed twice daily and any signs of disease or discomfort were reported to the veterinary staff for evaluation. At the end of the study, the NHPs were euthanized following procedures approved in the IACUC protocol.

Flow cytometry gating strategies. CD4⁺ and CD8⁺ T cell percentages were obtained by first gating on lymphocytes, then on CD3⁺ T cells. The relative proportion of CD4⁺ T cells in peripheral blood and intestinal samples was calculated as the "index" of baseline total CD4⁺ T cells at these sites (considering baseline as 100%) to more clearly represent the CD4⁺ T cell depletion. Memory CD4⁺ T cell subsets were defined based on the CD28 and CD95 expression as: naïve (CD28⁺ CD95^{neg}), central memory (CD28⁺ CD95⁺) and effector memory (CD28^{neg} CD95⁺) cells. T cell activation status (Glut-1⁺, HLA-DR⁺ CD38⁺, or Ki-67⁺) was assessed by gating on lymphocytes, then on CD3⁺ T cells, and finally on CD4⁺ CD3⁺ or CD8⁺ CD3⁺ T cells. CD14 and CD16 were used to identify circulating monocyte subsets and CD163 was used to identify intestinal macrophages, by gating first on the CD3^{neg} HLA-DR⁺ immune cell population. Monocyte/macrophage activation was

determined based on the expression of Glut-1, CD80 and CD86 on monocytes/macrophages. Regulatory T cells (Tregs) were defined as FoxP3⁺ CD25⁺ CD4⁺ CD3⁺ and FoxP3⁺ CD25⁺ CD8⁺ CD3⁺ populations.

The absolute CD3 T cell counts in peripheral blood were obtained with BD Trucount™ Tubes (BD Biosciences). The absolute counts of circulating CD4⁺ and CD8⁺ T cells were further calculated through gating on the lymphocytes and CD3⁺ T cells.

Immunohistochemistry. Briefly, for antigen retrieval and endogenous peroxidase blocking, the sections were microwaved in Vector Unmasking Solution (Vector Laboratories Burlingame, CA) and then treated with 3% hydrogen peroxide. Sections were first incubated with the primary antibodies (Table S3) for 1 hr at room temperature, then incubated with secondary antibodies (30 min), followed by incubation with an Avidin/Biotin complex (30 min), both included in the Vector Vectastain anti-mouse and anti-rabbit ABC Elite Kit. Sections were stained with 3,3-diamidino-benzidine (Dako Corporation, Carpinteria, CA) and counterstained with hematoxylin.

Measurement of plasma/serum LPS. Several factors present in plasma have been shown to interfere with LPS measurements (LBP, EndoCAb, HDL, plasma turbidity, proteins and triglycerides). Therefore, to minimize any possible interference, plasma samples were diluted 5-fold with endotoxin-free water and then heated to 85°C for 15 min to inactivate plasma proteins. Plasma LPS was then quantified with Limulus Amebocyte Lysate assay (Lonza, Walkersville, MD), according to manufacturer's protocol.

PBMC Metabolic Assays. Cells were used immediately after thawing rapidly in 37°C water bath and adhered at 7×10^5 cells per well onto wells of Cell-Tak (Corning) coated XF96 plate (Agilent

Technologies, Seahorse Bioscience). Oxygen consumption rate (OCR) and extracellular acidification rate (ECAR) were measured using the mitochondrial stress test procedure in XF base medium supplemented with 10 mM glucose (Sigma), 4 mM L-glutamine and 2 mM sodium pyruvate under basal conditions and in response to 1 μ M oligomycin (Agilent, Seahorse Bioscience), 1.5 μ M fluorocarbonyl cyanide phenylhydrazone FCCP (Agilent, Seahorse Bioscience) and 1 μ M Rotenone (Sigma) with the XF96 Extracellular Flux Analyzer (Agilent, Seahorse Bioscience). All measurements were normalized to cell numbers.

Supplemental Figures and Tables

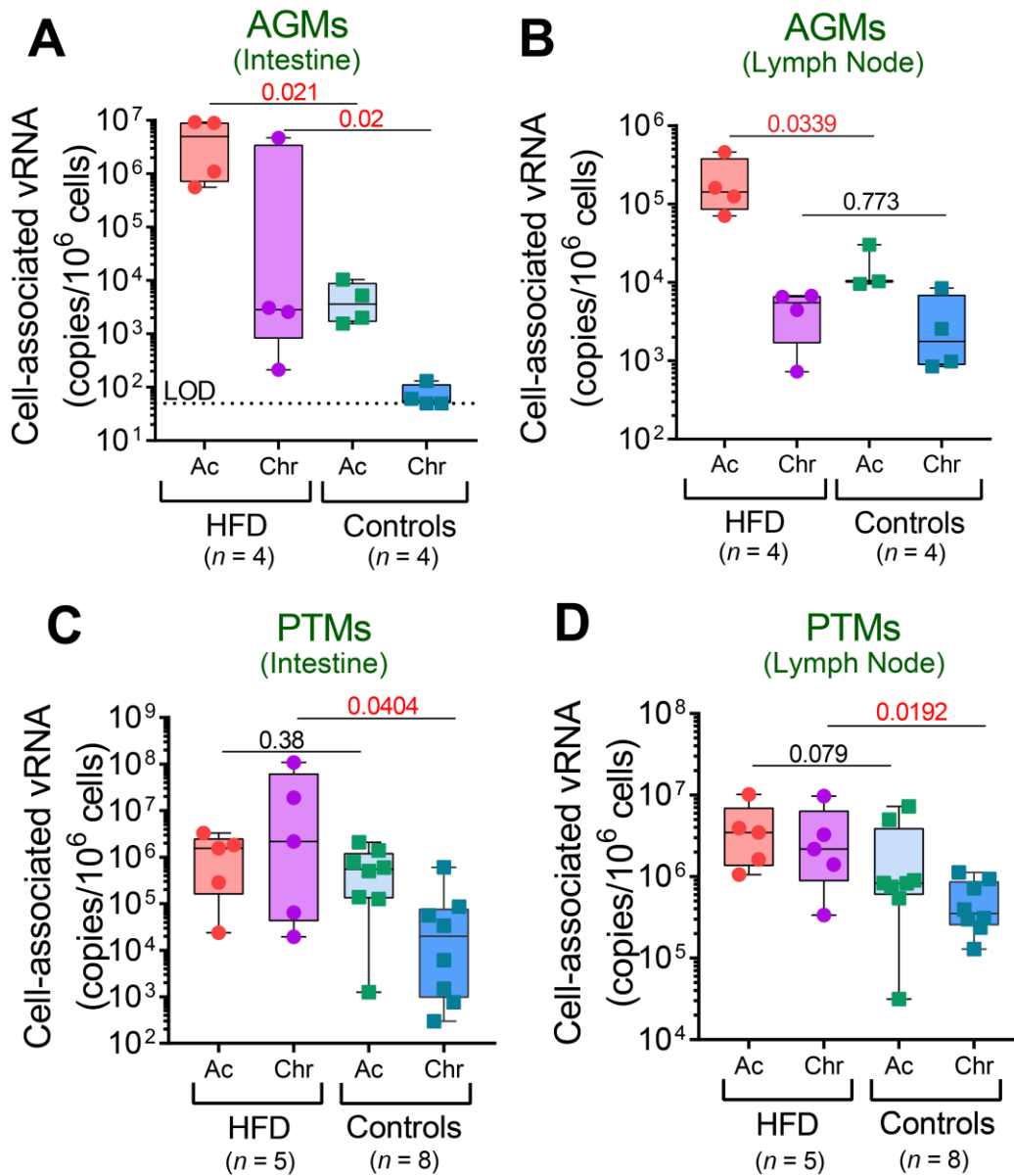


Figure S1. HFD-receiving NHPs have higher cell-associated SIV RNA in the intestine and the lymph nodes. Cell-associated RNA levels in the intestine (**A**) and in the lymph nodes (**B**) of SIV-infected AGMs, and in the intestine (**C**) and in the lymph nodes (**D**) of SIV-infected PTMs were compared at acute and chronic infection between HFD and control groups with Kruskal-Wallis test. Data are presented as individual values with medians. Sample size (*n*) and P-values are presented on graphs. Ac, acute infection; Chr, chronic infection.

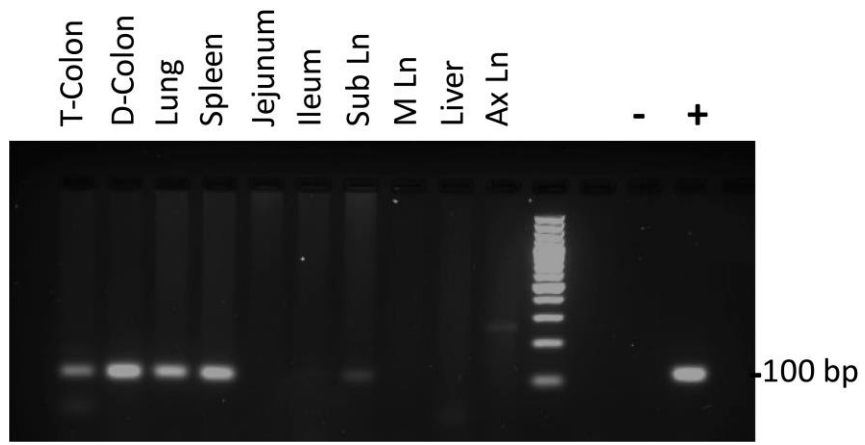


Figure S2. CMV identification in the tissues collected from the HFD-receiving AGM that died during the follow-up. CMV was detected in transverse and descendant colon, lung, spleen and in the submandibular lymph node.

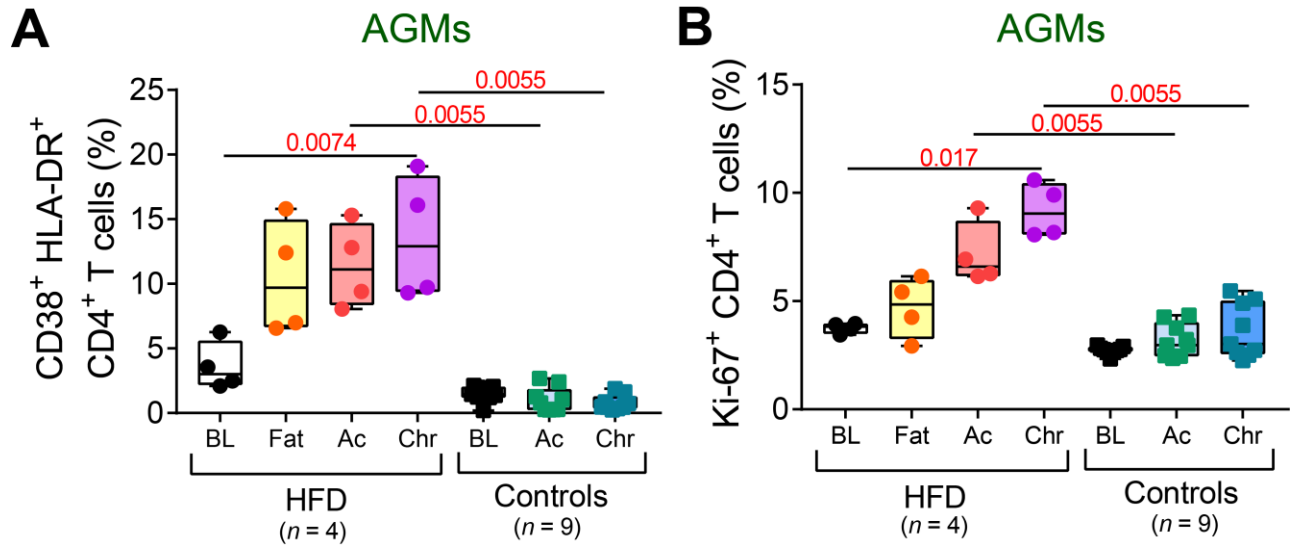


Figure S3. HFD increases the levels of CD4⁺ T cell activation in SIV-infected AGMs. Frequencies of CD4⁺ T cells coexpressing CD38 and HLA-DR (**A**), as well as CD4⁺ T cells expressing Ki-67 (**B**) in the peripheral blood of AGMs were compared at key time points of SIV infection within HFD group with Friedman test corrected for multiple comparisons, and between HFD and control groups with Kruskal-Wallis test. Data are presented as individual values with medians. Sample size (*n*) and P-values are presented on graphs. BL, baseline (preinfection pre-HFD); Fat, preinfection post-HFD; Ac, acute infection; Chr, chronic infection.

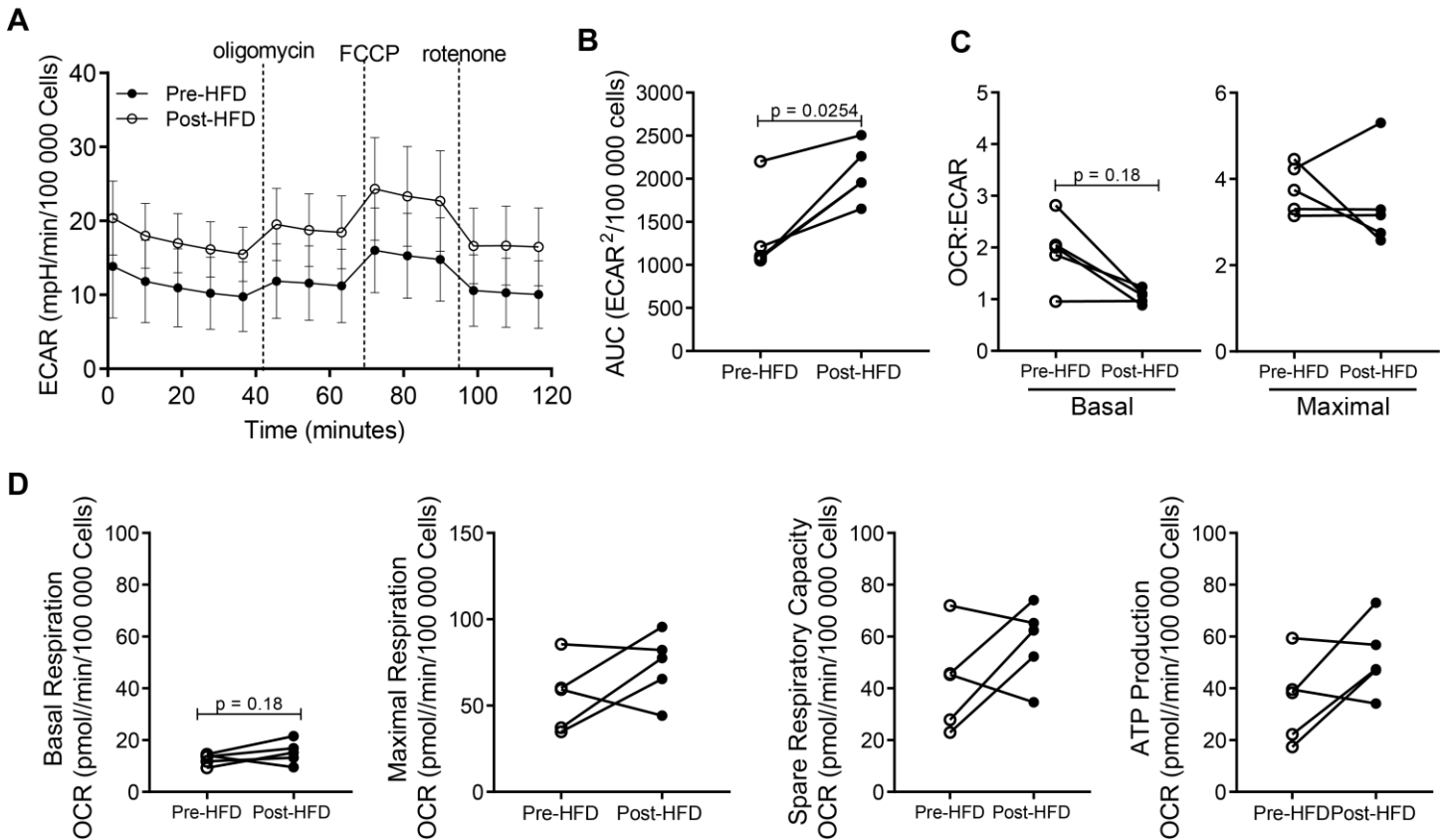


Figure S4. PBMCs of uninfected PTMs post-HFD administration have altered metabolic state. (A) Extracellular acidification rates (ECAR) and (B) area under the curve analysis of total peripheral blood mononuclear cells (PBMCs) from PTMs ($n = 5$) pre- and post-HFD. (C) Metabolic parameters and (D) oxygen consumption rate (OCR):ECAR ratio at basal and maximal respiration derived using the Seahorse analysis program for the Mito Stress test were compared for PBMCs collected pre- and post-HFD administration using Wilcoxon signed-rank test. Data are presented as means with SEM in panel (A), and as paired individual values in panels (B-D). Sample size (n) and P-values are presented on graphs.

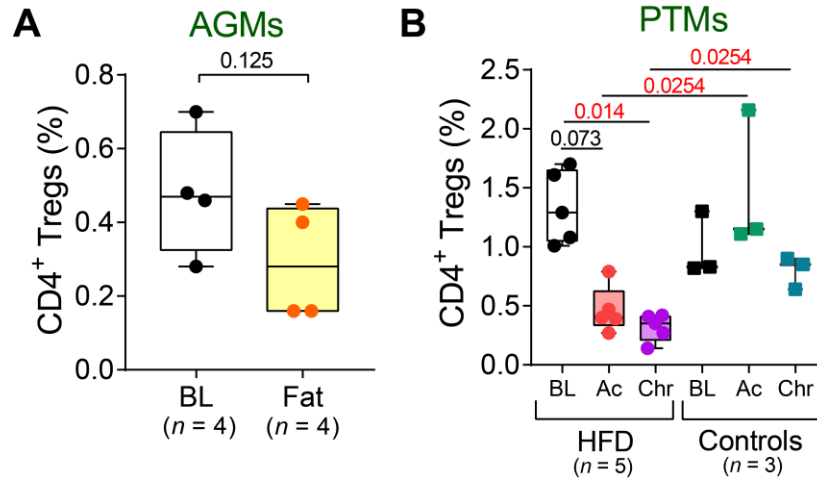


Figure S5. HFD decreases regulatory CD4⁺ T cells in the gut. (A) Frequencies of regulatory CD4⁺ T cells in the gut of uninfected AGMs are compared before and after HFD administration by Wilcoxon signed-rank test. (B) Frequencies of regulatory CD4⁺ T cells in the gut are compared between HFD-receiving PTMs and controls at key time points of SIV infection within HFD group with Friedman test corrected for multiple comparisons, and between HFD and control groups with Kruskal-Wallis test. Data are presented as individual values with medians. Sample size (*n*) and P-values are presented on graphs. BL, baseline (preinfection pre-HFD); Fat, preinfection post-HFD; Ac, acute infection; Chr, chronic infection.

Table S1. Histological findings and cause of death in HFD-receiving and control SIV-infected PTMs

Cause of death	
HFD1	<ul style="list-style-type: none"> •lesions indicative of AIDS with severe lymphoid depletion •giant cell disease •severe encephalitis •atypical Mycobacteria infection
HFD2	<ul style="list-style-type: none"> •lesions indicative of AIDS with severe lymphoid depletion •thrombotic microangiopathy (TMA) •interstitial pneumonia •atypical Mycobacteria infection
HFD3	<ul style="list-style-type: none"> •lymphoid hyperplasia •TMA •severe bronchopneumonia and lung stasis indicative of heart failure
HFD4	<ul style="list-style-type: none"> •massive lymphoid hyperplasia in the lymph nodes, gut, kidney, lung •interstitial pneumonia with nuclear inclusions •lung stasis indicative of heart failure •atypical Mycobacteria infection
HFD5	<ul style="list-style-type: none"> •lymphoid depletion characteristic to AIDS •massive lymph node fibrosis •foamy cells in the ileum, suggestive of atypical Mycobacteria infection •giant cell disease •brain lesions •lung stasis indicative of heart failure
CC1	<ul style="list-style-type: none"> •lesions of late-stage AIDS dominated by severe lymphoid depletion •pneumonia
CC2 (euthanized)	<ul style="list-style-type: none"> •compensated SIV infection dominated by massive lymphoid hyperplasia and lymphoid infiltrates and aggregated in all tissues
CC3 (euthanized)	<ul style="list-style-type: none"> •compensated SIV infection dominated by massive lymphoid hyperplasia and lymphoid infiltrates and aggregated in all tissues
HC1	<ul style="list-style-type: none"> •lesions indicative of late stage of SIV infection with a mixture of lymphoid hyperplasia and lymphoid depletion in lymph nodes •numerous lymphoid infiltrates in the lungs •TMA
HC2	<ul style="list-style-type: none"> •numerous liver granulomas indicative of atypical Mycobacterial infection •severe lymphoid infiltration of the lungs and adipose tissue •glomerulonephritis and lymphoid infiltration in the kidneys •severe lymphoid hyperplasia in some lymph nodes •other lymph nodes are atrophic, indicative for the onset of AIDS
HC3	<ul style="list-style-type: none"> •extensive lymphoid infiltrates in the lung, kidney and jejunum •lymphoid hyperplasia of superficial and mesenteric lymph nodes with confluent germinal centers •TMA
HC4	<ul style="list-style-type: none"> •lymphoid depletion and severe fibrosis of the lymph nodes •mixture of lymphoid hyperplasia and lymphoid depletion in the jejunum •glomerulonephritis, hyaline deposits in the kidneys, TMA, arteritis •liver granulomas indicative of atypical Mycobacterial infection
HC5	<ul style="list-style-type: none"> •giant cell disease indicative of AIDS •interstitial pneumonia, complicated with bacterial infection •encephalitis •lymphoid depletion and severe fibrosis of the lymph nodes
HC6	<ul style="list-style-type: none"> •lymphoid depletion of the lymph nodes and colon with collagen deposition in both sides indicative of AIDS •CMV interstitial pneumonia complicated with bacterial infection •TMA
HC7	<ul style="list-style-type: none"> •encephalitis •B cell Lymphoma •arteritis •TMA

^A HFD1-5, high fat diet-receiving PTMs; CC1-3, contemporary control PTMs; HC1-7, historical control PTMs.

Table S2. Cardiovascular lesions in HFD-receiving and control SIV-infected PTMs

	Myocardial inflammation	Large necrotic areas	Microthrombi	Pericardial inflammation	Abdominal aorta ATS	Coronaries ATS	Coronaries inflammation	Steatosis/Fatty infiltration
HFD1	5	+	6	4	0	0	4	3
HFD2	7	0	3	10	2	0	4	2
HFD3	4	+	6	3	1	0	6	4
HFD4	7	+	0	3	1	1	2	0
HFD5	5	0	0	2	1	0	4	0
CC1	3	0	2	2	0	0	2	0
CC2	3	0	0	2	0-1	0	0	0
CC3	4	+	0	2	0	0	0	0
HC1	5	+	0	2	1	ND	ND	0
HC2	7	+	3	5	0	ND	ND	0
HC3	1	0	3	2	1	ND	ND	0
HC4	1	0	2	3	0	ND	ND	0
HC5	5	+	3	6	0	ND	ND	2
HC6	0	0	0	0	0	ND	ND	0
HC7	1	0	1	1	ND	1	0	0

^A HFD1-5, high fat diet-receiving PTMs; CC1-3, contemporary control PTMs; HC1-7, historical control PTMs. ND, not determined. Cardiovascular lesions are scored on a scale of 0-10 based on their severity, except for necrotic areas, which is presented as present (+) or not present (0).

Table S3. Antibodies used for flow cytometry assay

Marker	Clone	Company	Usage
CD3	SP34-2	BD Biosciences	Flow cytometry
CD4	L200	BD Biosciences	Flow cytometry
CD8	RPA-T8	BD Biosciences	Flow cytometry
CD28	CD28.2	BD Biosciences	Flow cytometry
CD95	DX2	BD Biosciences	Flow cytometry
CD38	HB7	BD Biosciences	Flow cytometry
HLA-DR	L243	BD Biosciences	Flow cytometry
Ki-67	B56	BD Biosciences	Flow cytometry
CD14	M5E2	BioLegend	Flow cytometry
CD16	3G8	BD Biosciences	Flow cytometry
CD163	GHI/61	BioLegend	Flow cytometry
Glut-1	SLC2A1	Novus Biologicals	Flow cytometry
CD80	L307.4	BD Biosciences	Flow cytometry
CD86	2331(FUN-1)	BD Biosciences	Flow cytometry
IL-17	eBio64CAP17	Invitrogen	Flow cytometry
FoxP3	259D	BioLegend	Flow cytometry
CD25	2A3	BD Biosciences	Flow cytometry
Myeloperoxidase	Polyclonal	Dako	Immunohistochemistry
Cytomegalovirus	CCH2+DDG9	Dako	Immunohistochemistry